Title

Ultrastructure Expansion Microscopy (U-ExM) in *Trypanosoma cruzi*: localization of tubulin isoforms and isotypes

Author and Affiliation

Victoria Lucia Alonso[1,2] *

[1] Instituto de Biología Molecular y Celular de Rosario, CONICET. Rosario, Argentina.

[2] Facultad de Ciencias Bioquímicas y Farmacéuticas, Universidad Nacional de Rosario. Rosario, Argentina.

*Corresponding author

Abstract

Ultrastructure Expansion Microscopy (U-ExM) is a recently developed technique that enables the increase of the spatial resolution within a cell or a tissue for microscopic imaging by physically expanding the sample. I report, for the first time, a detailed protocol validating the use of U-ExM in *Trypanosoma cruzi* and quantifying the expansion factors of different subcellular compartments. I was able to determine the localization patterns of different tubulin isoforms, such as α-tubulin and β-tubulin. Also, I immunolocalized acetylated and tyrosinated α-tubulin isotypes in epimastigotes and use mitochondrial cell-permeable dyes to identify this organelle. Finally, U-ExM was also performed in trypomastigotes and amastigotes validating this technique in all life cycle stages of *T. cruzi*.

Keywords

Confocal microscopy, cytoskeleton, acetylation, tyrosination, mitochondria

29 **Introduction**

30 *Trypanosoma cruzi*, the etiological agent of Chagas disease or American trypanosomiasis, is a
31 kinetoplastid parasite with a complex life cycle that alternates between a mammalian and an insect
32 host (Triatominidae family), which is the biological vector of this disease (Lidani et al. 2019).
33 The World Health Organization classifies Chagas disease as one of the 13 most neglected tropical
34 diseases, constituting a very important social and economic problem, especially in Latin America.
35 The cytoskeleton of trypanosomatids has a simpler arrangement than most eukaryotic cells, but it
36 is precisely organized and constituted by stable microtubules (MT). Such MTs compose the
37 mitotic spindle, the basal body, the flagellar axoneme, and the subpellicular microtubules, which
38 are connected to each other and to the plasma membrane, thus forming a helical arrangement
39 along the central axis of the parasite cell body (de Souza 2009). MTs provide the basis for
40 cytoskeletal architecture and are formed by α/β-tubulin heterodimers forming helical tubes. They
41 are regulated by interacting with a variety of MT-associated proteins (MAPs), by a differential
42 expression of α- and β-tubulin genes (tubulin isotypes), and by tubulin isoforms generated by the
43 inclusion of a variety of post-translational modifications (PTMs) in each isotype (Gadadhar et al.
44 2017). In trypanosomatids, many PTMs were identified across the microtubular array. It is
45 proposed that this could be used to control the differential recruitment of MAPs and motors during
46 the cell cycle (Sinclair and de Graffenried 2019).

47 Ultrastructure Expansion microscopy (U-ExM) is a recently introduced super-resolution
48 microscopy technique in which swellable polymer hydrogels are used to physically expand fixed
49 biological specimens to resolve fine details (Chen et al. 2015). The method is particularly
50 attractive due to its simplicity and accessibility, its compatibility with conventional fluorescent
51 probes, and inexpensive chemicals. It can achieve a spatial resolution of ~65 nm using
52 conventional (confocal) microscopes, approximately four times better than that of the same
53 microscope alone (~250 nm).

54 Since 2015 there has been a steady growth of the publication involving this technique, especially
55 in protozoan parasites, like *Giardia lamblia*, *Plasmodium falciparum,* and *Toxoplasma gondii*
56 (Tillberg and Chen 2019; dos Santos Pacheco and Soldati-Favre 2021; Gorilak et al. 2021;

57 Tomasina et al. 2021). The use of ultrastructure expansion microscopy was first demonstrated in
58 Kinetoplastea localizing a component of the mitochondrial genome segregation machinery in
59 *Trypanosoma brucei* (Amodeo et al. 2021; Kalichava and Ochsenreiter 2021) but it has not been
60 reported in *T. cruzi*.
61 In this report, I validate the use of U-ExM in *Trypanosoma cruzi* and quantify the expansion
62 factors of different subcellular structures. I describe the localization patterns of tubulin isoforms,
63 such as α-tubulin, β-tubulin, validating this technique in all life cycle stages of *T. cruzi*. Also, I
64 immunolocalized acetylated and tyrosinated α-tubulin isotypes in epimastigotes to visualize
65 subpellicular microtubules, the flagellar axoneme, the basal body, and the flagellar pocket.
66 Furthermore, I validated the use of the cell-permeable dyes, such as Mitotracker, for U-ExM in
67 *T. cruzi*.

68 **Methods**

69 Parasite culture and infections

70 *T. cruzi* Dm28*c* epimastigotes and Vero cells (ATCC CCL-81) were cultured and infected as
71 previously described (Alonso et al. 2016).

72 U-ExM protocol

73 5 million epimastigotes or trypomastigotes were washed twice with 500 µl PBS and centrifuged
74 for 5 min at 2000 g, then resuspended in 200 µl of PBS and settled for 20 min at room temperature
75 on poly-D-lysine coated coverslips (12 mm, Marlenfeld GmbH). For mitochondrial staining,
76 epimastigotes were resuspended in PBS and incubated with 1mM Mitotracker Orange CMTMRos
77 (Invitrogen) for 30 min at 28°C, washed twice in PBS and fixed with
78 3% paraformaldehyde + 0.1% Glutaraldehyde (Sigma, 70% solution) in PBS for 15 min at RT and
79 then settled on coverslips as described before. Cells infected with amastigotes in 12 mm
80 coverslips were washed twice with PBS to eliminate culturing. For all the conditions stated above,
81 coverslips were carefully submerged into a 24-well plate with 1 ml of 4% Formaldehyde (FA,
82 36.5–38%, Sigma) and 4% acrylamide (AA, 40% stock solution, Invitrogen) in PBS and
83 incubated for four to five hours at 37°C. For gelation, coverslips were putted, with the cells facing

84 down, into 35µl of monomer solution: 19% Sodium Acrylate (Sigma), 10% AA, 0.1% N, N'-
85 methylenbisacrylamide (BIS, Sigma) in PBS, supplemented with 0.5% APS (Sigma) and 0.5%
86 tetramethylethylenediamine (TEMED, Sigma). Drops of monomer solution were placed over a
87 parafilm in a pre-cooled humid chamber. Gelation proceeded for 5 mins on ice, and then samples
88 were incubated at 37°C in the dark for 1 h. Coverslips with gels were then transferred into a six-
89 well plate filled with 2 ml of denaturation buffer (200 mM sodium dodecyl sulfate (SDS), 200
90 mM NaCl, and 50 mM Tris-HCl in MilliQ, pH 9) for 15 min at room temperature with gentle
91 agitation to allow the gels to detach from the coverslips. Gels were then moved into a 1.5 ml
92 Eppendorf centrifuge tube filled with 1 ml denaturation buffer and incubated at 95°C for 1 h and
93 30 min. After denaturation, gels were placed in 50 ml beakers or Petri dishes filled with MilliQ
94 water for the first round of expansion. Water was exchanged after 30 minutes and then gels were
95 incubated overnight in MilliQ water. The next day, water was exchanged one more time for 30
96 minutes and then gels were washed two times for 30 min in PBS (gel shrinkage) and subsequently
97 incubated with primary antibody (Table I), all antibodies were diluted in 2% PBS/BSA, and gels
98 were incubated for 3 h at 37°C and then overnight at 4ºC in 24 well plates with 300 µl of the
99 diluted antibodies. Gels were then washed in PBS-T three times for 10 min while gently shaking
100 and subsequently incubated with secondary antibodies (Table I) using the same incubation times.
101 The day after, gels were washed in PBS-T (three times for 10 min while shaking) and placed into
102 beakers or Petri dishes filled with MilliQ water for the second round of expansion. Water was
103 exchanged three times every 30 min. After this step, gels were carefully measured with a caliper
104 showing an expansion factor between 4.2x and 4.6x. The specificity of the antibodies was verified
105 by western blot with epimastigotes' total extracts (Figure 1a).

106 Imaging and measurement of the expansion

107 The gel was then cut with a razor blade into pieces and put into a 35 mm glass-bottom dish
108 (Matsunami) previously coated with poly-lysine for confocal imaging. Confocal microscopy was
109 performed on a Zeiss LSM880 using a 63x oil NA 1.4 objective, with the following parameters:
110 z step size at 0.65 µm interval with a pixel size of 0.132 nm. ZEN BLACK 2.1 SP3 software

111 (Zeiss, RRID:SCR_018163) and Fiji (Schindelin et al. 2012) (RRID:SCR_002285) were used to
112 analyze the images.
113 The expansion factor was determined by comparing the ratio of expanded kinetoplast and nucleus
114 to non-expanded epimastigotes (n = 20 cells). Statical analysis of these measurements was
115 performed with GraphPad Prism v. 9.0.1 (RRID:SCR_002798). The length of the kinetoplast was
116 determined by measuring its maximum length. The diameter of the nucleus was determined by
117 measuring the widest diameter observed in each epimastigote using Fiji.

118 **Results and Discussion**

119 U-ExM workflow in *T. cruzi*

120 Although the Ex-M protocols present in the literature follow the same steps, they have differences
121 regarding the concentration of fixative agents, denaturing agents, and incubation times (this also
122 depends on the nature of the protein to be immunolocalized). I tested several conditions and
123 optimized the workflow for *T. cruzi* (Figure 1), which is described in Methods section. In this
124 report, I used antibodies against cytoskeletal proteins (insoluble proteins) (Table I) and gave a
125 detailed protocol to perform the U-ExM, but is important to mention that the incubation time
126 when targeting soluble proteins or membrane proteins the incubation time and temperature during
127 the denaturing step should be optimized.
128 As observed in Figure 1, in the first step, the precursor molecules FA and AA are introduced to
129 functionalize the cellular components allowing the subsequent linkage of swellable
130 polyelectrolyte gel (Monomer solution containing SA). The gel formation is accomplished using
131 the oxidizing reagents TEMED and APS, the same as for polyacrylamide gels. After the gel is
132 formed, the parasite contents are denatured using SDS and high temperature. Then, the first round
133 of expansion is performed in ultrapure water followed by incubation in PBS, where the gel shrinks
134 again. After this step, the sample is subjected to standard immunofluorescence techniques.
135 Finally, the second round of expansion in water is necessary before imaging in an epifluorescence
136 or confocal microscope.

137 Localization of tubulin isoforms

138 Alpha- and β-tubulin are fundamental components of the eukaryotic cytoskeleton and cell
139 division machinery. I immunolocalized these proteins using specific monoclonal antibodies
140 (Figures 2a and 2b). A similar localization pattern was observed for both isoforms at the
141 subpellicular microtubules and the flagellar axoneme (from the base of the flagellum to its tip
142 revealing its continuous attachment to the cell body as previously described (de Souza 2009)).
143 Pro-and mature basal bodies were also detected with their associated microtubule quartet in
144 proximity to the kinetoplast in a parasite that is starting to divide (Zoom in Figure 2b) (Elias et
145 al. 2007).
146 Alpha-tubulin was also immunolocalized in trypomastigotes and amastigotes highlighting the
147 value of this technique in all life cycle stages of *T. cruzi*. As observed in figure 2c the subpellicular
148 array and the flagellar axoneme are clearly immunostained in both stages. It is interesting to note
149 that the anti α-tubulin antibody used (TAT-1), immunodetects, in our experimental conditions,
150 exclusively amastigotes' α-tubulin and not the host cell protein, I believe this is because TAT-1
151 was developed by immunizing mice with extracted *T. brucei brucei* cytoskeleton although it is
152 suitable to use in mammalian cells.
153 Localization of tubulin isotypes in *T. cruzi*
154 Several conserved lysines (K) in α- and β-tubulin are acetylated, and acetylation of the α-tubulin
155 luminal residue K40 has been the most characterized since its discovery over thirty years ago.
156 This PTM is associated with microtubules stability and a marker of resistant microtubules to
157 depolymerizing drugs (L'Hernault and Rosenbaum 1985). Subpellicular, mitotic and axonemal
158 microtubules are extensively acetylated in Trypanosomatids, which makes these organisms
159 interesting models for studying K40 acetylation (Sasse and Gull 1988; Souto-Padron et al. 1993).
160 The immunolocalization of acetylated α-tubulin in the subpellicular microtubules and flagellar
161 axoneme is observed in great detail using U-ExM, it can also be observed flagellar pocket (Figure
162 3a) and basal body staining. Tyrosinated α-tubulin shows a different localization pattern (Figure
163 3b), the subpellicular MTs of the posterior third of the cell body, the nascent daughter flagellum of
164 dividing cells, and the basal bodies all react strongly, similar to the localization in *T. brucei* (Sherwin

165 et al. 1987). A weak reaction is detected in the subpellicular MTs of the anterior two-thirds of the cell
166 body and the old flagellum.

167 Measurement of subcellular compartments and structures in epimastigotes

168 Trypanosomatids are characterized by a single flagellum and a mass of mitochondrial DNA
169 organized into a kinetoplast connected to the proximal end of the basal bodies and the flagellar
170 pocket (Gull 1999). The kinetoplast was measured in epimastigotes stained with Mitotracker and
171 for nuclear measurements, I stained epimastigotes' DNA with DAPI (Figure 3c). With
172 Mitotracker staining, the ramifications of the single mitochondria of *T. cruzi* are clearly identified
173 and the kinetoplast is deeply marked, this also allowed us to validate the use of cell-permeable
174 dyes for U-ExM in *T. cruzi*. Using DAPI I was able to discriminate condensed regions of the
175 chromatin as well as the nucleolar domain (identified by the lack of DAPI staining) (Figure 3c).
176 An expansion factor of 4.2x and 4.6x was quantified for the nucleus and the kinetoplast
177 respectively, which signifies that expansion was homogeneous within the cells (Figure 3d).
178 When compared with non-expanded epimastigotes, the resolution gain is clear and allowed us to
179 visualize the potential of this technique in *T. cruzi* (Figure 3e). In conclusion, U-ExM is a
180 powerful approach for studying cytoskeletal structures in *T. cruzi*. It is a robust super-resolution
181 method, but very simple, and does not need highly specialized reagents or instrumentation. U-
182 ExM allows high-resolution imaging, improving the axial and lateral effective resolution of the
183 molecules to be analyzed. An expansion factor of four increases resolution from around 250 nm
184 to less than 70 nm using regular confocal microscopy. In the future, this could be further improved
185 by super-resolution techniques to visualize biomolecular structures that are in close proximity to
186 each other, such as the components of the flagellar pocket and basal body.

187 **Statements and Declarations**

188 Competing interest

189 The authors have no relevant financial or non-financial interests to disclose.

190 Funding

This work was supported by Agencia Nacional de Promoción Cientifica y Tecnológica from Argentina (PICT2017-1978 and PICT2019-0526) and the Research Council United Kingdom (MR/P027989/1).

Authors contribution statement.

VLA has designed, performed the experiments, and wrote the manuscript.

Acknowledgments.

Thanks to Dr. Esteban Serra and Dr. Luis E. Tavernelli for the critical reading of the manuscript. I am also very grateful to Rodrigo Vena for assisting in the acquisition of confocal images.

References

Alonso VL, Ritagliati C, Cribb P, et al (2016) Overexpression of bromodomain factor 3 in Trypanosoma cruzi (Tc BDF3) affects parasite differentiation and protects it against bromodomain inhibitors. FEBS Journal 283:2051–2066. https://doi.org/10.1111/febs.13719

Amodeo S, Kalichava A, Fradera-Sola A, et al (2021) Characterization of the novel mitochondrial genome segregation factor TAP110 in Trypanosoma brucei. Journal of Cell Science 134:. https://doi.org/10.1242/JCS.254300/237572

Chen F, Tillberg PW, Boyden ES (2015) Expansion Microscopy. Science (New York, NY) 347:543. https://doi.org/10.1126/SCIENCE.1260088

de Souza W (2009) Structural organization of Trypanosoma cruzi. Memórias do Instituto Oswaldo Cruz 104 Suppl:89–100

dos Santos Pacheco N, Soldati-Favre D (2021) Coupling Auxin-Inducible Degron System with Ultrastructure Expansion Microscopy to Accelerate the Discovery of Gene Function in Toxoplasma gondii. Methods in molecular biology (Clifton, NJ) 2369:121–137. https://doi.org/10.1007/978-1-0716-1681-9_8

Elias MC, da Cunha JPC, de Faria FP, et al (2007) Morphological Events during the Trypanosoma cruzi Cell Cycle. Protist 158:147–157. https://doi.org/10.1016/j.protis.2006.10.002

Gadadhar S, Bodakuntla S, Natarajan K, Janke C (2017) The tubulin code at a glance. Journal of Cell Science 130:1347–1353. https://doi.org/10.1242/jcs.199471

218 Gorilak P, Pružincová M, Vachova H, et al (2021) Expansion microscopy facilitates quantitative
219 super-resolution studies of cytoskeletal structures in kinetoplastid parasites. Open Biology
220 11:. https://doi.org/10.1098/RSOB.210131
221 Gull K (1999) The cytoskeleton of trypanosomatid parasites. Annual review of microbiology
222 53:629–655
223 Kalichava A, Ochsenreiter T (2021) Ultrastructure expansion microscopy in Trypanosoma brucei.
224 Open Biology 11:. https://doi.org/10.1098/RSOB.210132
225 L'Hernault SW, Rosenbaum JL (1985) Chlamydomonas .alpha.-tubulin is posttranslationally
226 modified by acetylation on the .epsilon.-amino group of a lysine. Biochemistry 24:473–478.
227 https://doi.org/10.1021/bi00323a034
228 Lidani KCF, Andrade FA, Bavia L, et al (2019) Chagas Disease: From Discovery to a Worldwide
229 Health Problem. Frontiers in Public Health 7:1–13.
230 https://doi.org/10.3389/fpubh.2019.00166
231 Sasse R, Gull K (1988) Tubulin post-translational modifications and the construction of
232 microtubular organelles in Trypanosoma brucei. Journal of Cell Science 90:577 LP – 589
233 Schindelin J, Arganda-Carreras I, Frise E, et al (2012) Fiji: an open-source platform for
234 biological-image analysis. Nature methods 9:676–682.
235 https://doi.org/10.1038/NMETH.2019
236 Sherwin T, Schneider A, Sasse R, et al (1987) Distinct localization and cell cycle dependence of
237 COOH terminally tyrosinated alpha-tubulin in the microtubules of Trypanosoma brucei
238 brucei. J Cell Biol 104:439–446
239 Sinclair AN, de Graffenried CL (2019) More than Microtubules: The Structure and Function of
240 the Subpellicular Array in Trypanosomatids. Trends in Parasitology 35:760–777
241 Souto-Padron, Narcisa LCES, De Sousa W (1993) Acetylated alpha-tubulin in Trypanosoma
242 cruzi: inmunocytochemical localization. 88:517–528
243 Tillberg PW, Chen F (2019) Expansion Microscopy: Scalable and Convenient Super-Resolution
244 Microscopy. https://doi.org/101146/annurev-cellbio-100818-125320 35:683–701.
245 https://doi.org/10.1146/ANNUREV-CELLBIO-100818-125320

246 Tomasina R, González FC, Francia ME, et al (2021) Structural and Functional Insights into the
247 Microtubule Organizing Centers of Toxoplasma gondii and Plasmodium spp.
248 Microorganisms 2021, Vol 9, Page 2503 9:2503.
249 https://doi.org/10.3390/MICROORGANISMS9122503
250

251 **Fig. 1 a)** Specificity of the anti- α-tubulin, β-tubulin, acetylated (Ac) α-tubulin and tyrosinated
252 (Tyr) α-tubulin antibodies was verified by western blot against total epimastigotes extracts. 1
253 million parasites were blotted per lane, goat anti-mouse IgG conjugated to HRP was used as the
254 secondary antibody. **b)** U-ExM workflow in *T. cruzi*. Servier Medical Art was used to create this
255 figure (smart.servier.com)

256 **Fig. 2 Tubulin isotypes during *T. cruzi* cell stages a)** Epimastigotes stained with anti α-tubulin
257 antibodies (greyscale or magenta; Alexa 555) and DAPI (cyan; kDNA and nuclear DNA). In
258 Zoom images: bb, basal body; k, linetoplast; n, nucleus **b)** Epimastigotes stained with anti β-
259 tubulin antibodies (greyscale or magenta; Alexa 555) and DAPI (cyan; kDNA and nuclear DNA).
260 In Zoom images: bb, basal body; pro-bb, pro basal body; k, kinetoplast; n, nucleus, F, flagella **c)**
261 Trypomastogotes (T) and amastigotes (A) stained with anti α-tubulin antibodies (magenta; Alexa
262 555) and DAPI (cyan; kDNA and nuclear DNA).

263 **Fig. 3 Tubulin isoforms, mitochondrial staining and expansion measurments in**
264 **epimastigotes a)** Epimastigotes stained with anti Acetylated (Ac) α-tubulin antibodies (greyscale
265 or magenta; Alexa 555) and DAPI (cyan; kDNA and nuclear DNA). In Zoom images: bb, basal
266 body; F, flagella **b)** Epimastigotes stained with anti Tyrosonated (Tyr) a-tubulin antibodies
267 (greyscale or magenta; Alexa 555) and DAPI (cyan; kDNA and nuclear DNA). In Zoom images:
268 bb, basal body; F, flagella **c)** Epimastigotes stained with the cell-permeable dye Mitotracker and
269 DAPI. In Zoom images: k, kinetoplast; n, nucleus; nuc, nucleolus **d)** Nucleus and kinetoplast
270 measurements in expanded and non-expanded epimastigotes using Fiji. Expansion factor was
271 calculated as the ratio between non-expanded and expanded measurements **e)** Non-expanded and
272 expanded epimastigotes stained with anti α-tubulin (greyscale; Alexa 555).

Fig 1

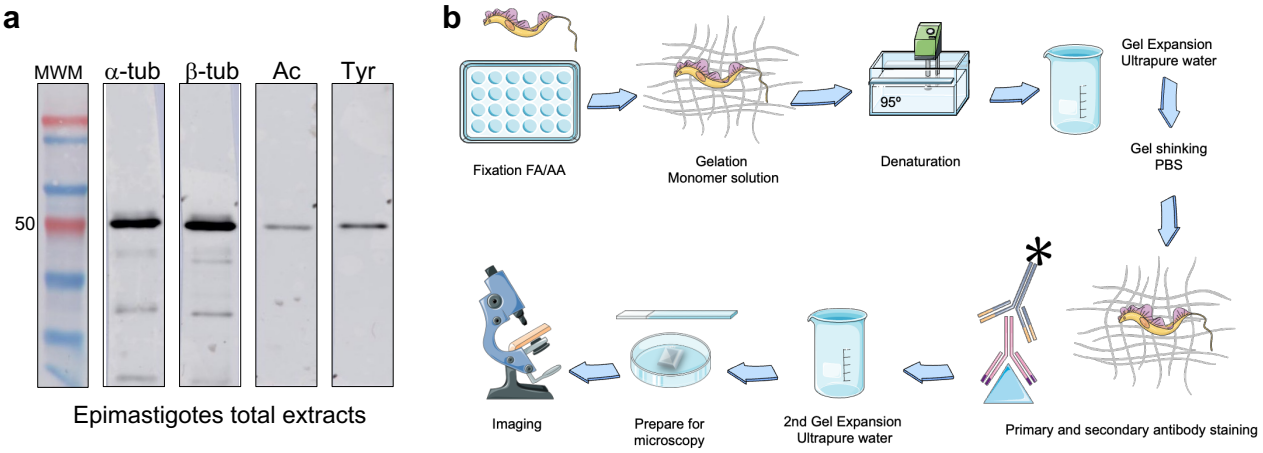
a
MWM
α-tub
β-tub
Ac
Tyr
50
Epimastigotes total extracts
b
Fixation FA/AA
Gelation
Monomer solution
95º
Denaturation
Gel Expansion
Ultrapure water
Gel shinking
PBS
Primary and secondary antibody staining
2nd Gel Expansion
Ultrapure water
Prepare for
microscopy
Imaging

Fig 2

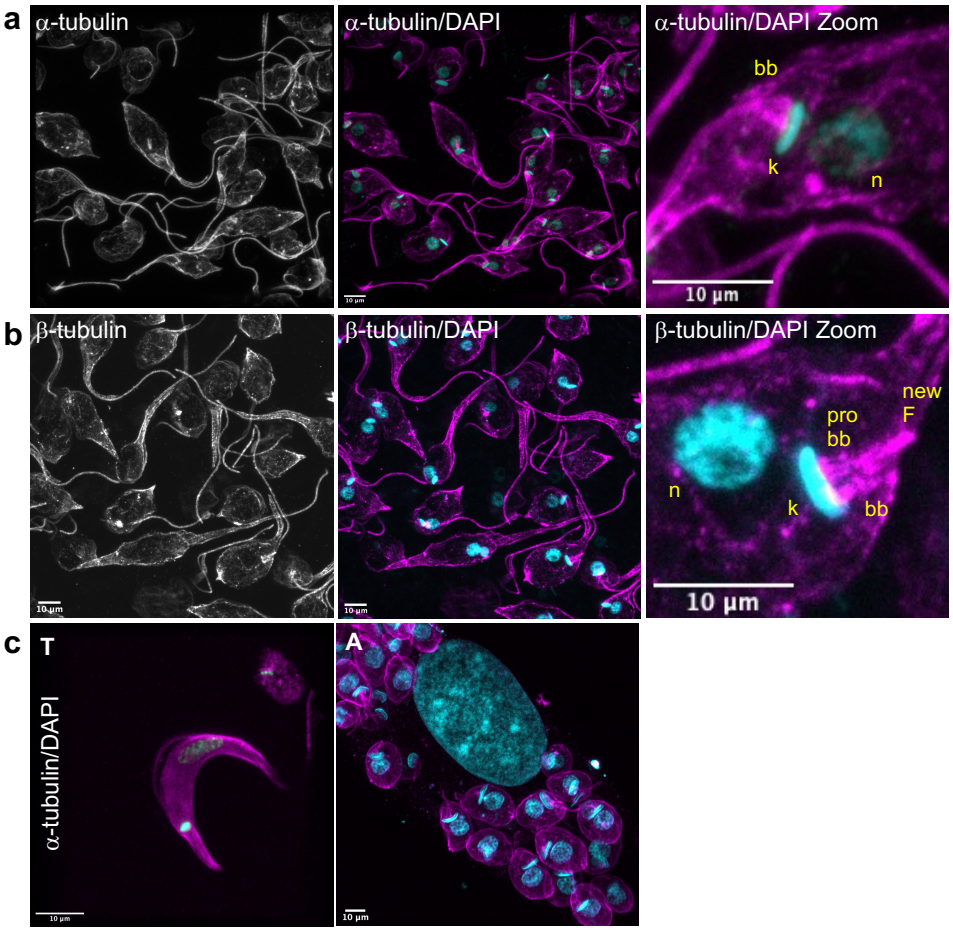
a
α-tubulin
α-tubulin/DAPI
α-tubulin/DAPI Zoom
bb
k
n
10 µm
b
β-tubulin
β-tubulin/DAPI
β-tubulin/DAPI Zoom
new
F
pro
bb
n
k
bb
10 µm
c
T
α-tubulin/DAPI
A
10 µm

Fig 3

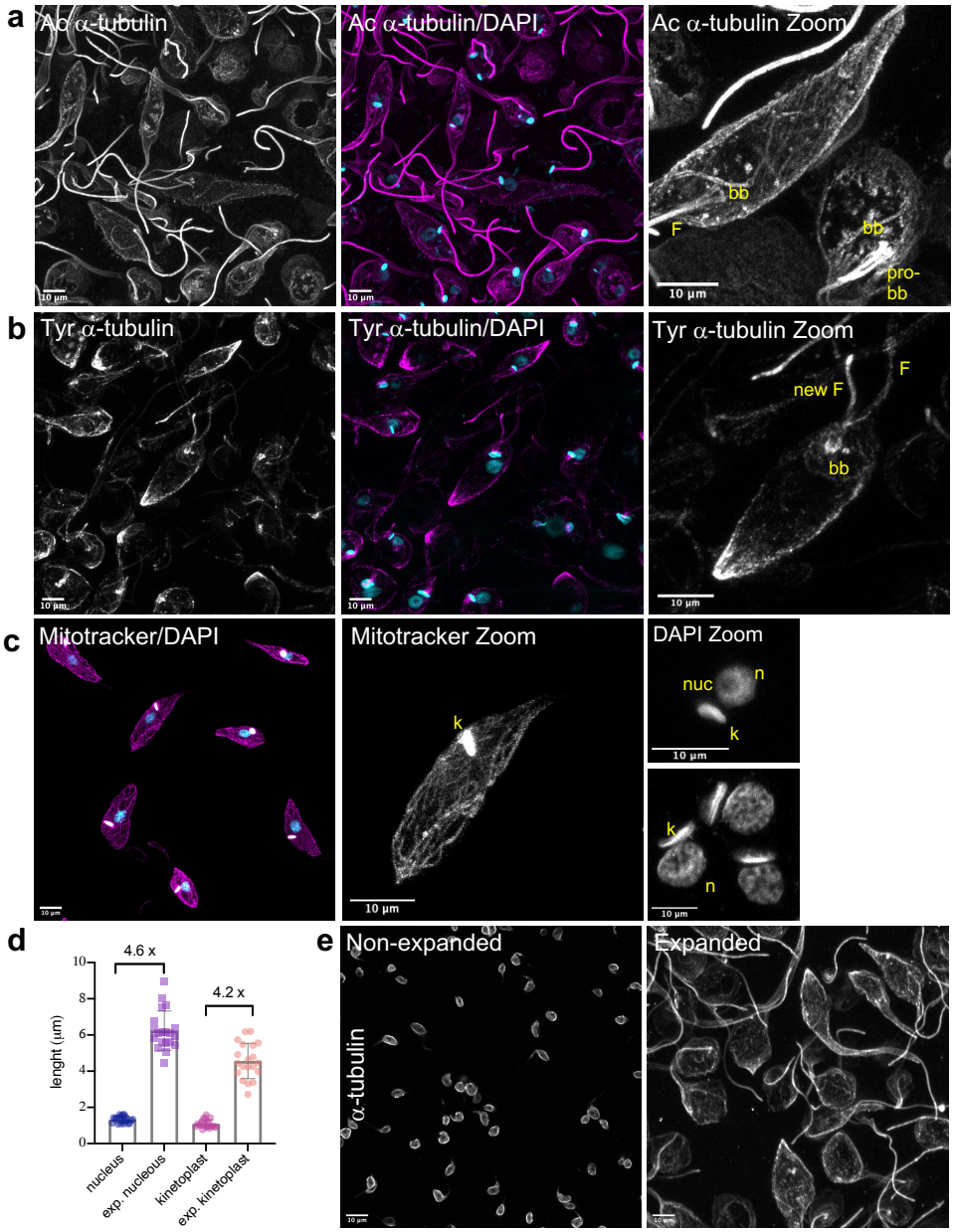
a
Ac α-tubulin
Ac α-tubulin/DAPI
Ac α-tubulin Zoom
bb
F
bb
pro-
bb
10 µm
b
Tyr α-tubulin
Tyr α-tubulin/DAPI
Tyr α-tubulin Zoom
F
new F
bb
10 µm
c
Mitotracker/DAPI
Mitotracker Zoom
k
10 µm
DAPI Zoom
nuc
n
k
10 µm
k
n
10 µm
d
4.6 x
4.2 x
lenght (µm)
10
8
6
4
2
0
nucleus
exp. nucleous
kinetoplast
exp. kinetoplast
e
Non-expanded
Expanded
α-tubulin
10 µm

Table I: List of antobodies used and working dilutions

Primary antibody	Target	Sourse	Recommended dilution ExM	Research Resource Identifiers (RRID
TAT-1	α-tubulin	Sigma Aldrich	1:200	Sigma-Aldrich Cat# 00020911, RRID:AB_10013740
KMX-1	β-tubulin	Millipore	1:200	Millipore Cat# MAB3408, RRID:AB_94650
YL1/2	α-tubulin tyrosinated	Millipore	1:300	Millipore Cat# MAB1864, RRID:AB_2210391
6-11B-1	α-tubulin acetylated	Sigma Aldrich	1:300	Sigma-Aldrich Cat# MABT868, RRID:AB_2819178
Secondary antibody				
anti-mouse Alexa 555	mouse IgG	Thermo Fisher	1:400	Thermo Fisher Scientific Cat# A-21427, RRID:AB_2535848